

Conjugate Bayes for probit regression via unified skew-normals

Daniele Durante

Bocconi University, Department of Decision Sciences, Via Roentgen 1, Milan, Italy

E-mail: daniele.durante@unibocconi.it

Summary. Regression models for dichotomous data are ubiquitous in statistics. Besides being fundamental for inference on binary responses, such representations additionally provide an essential building-block in more complex formulations, such as predictor-dependent mixture models, deep neural networks, graphical models, and others. Within a Bayesian framework, inference typically proceeds by updating the Gaussian priors for the regression coefficients with the likelihood induced by a probit or logit model for the observed binary response data. The apparent absence of conjugacy in this Bayesian updating has motivated a wide variety of computational methods, including Markov Chain Monte Carlo (MCMC) routines and algorithms for approximating the posterior distribution. Although such methods are routinely implemented, data augmentation MCMC faces convergence and mixing issues in imbalanced data settings and in hierarchical models, whereas approximate routines fail to capture the skewness and the heavy tails typically observed in the posterior distribution of the coefficients. This article shows that the posterior for the coefficients of a probit model is indeed analytically available—under Gaussian priors—and coincides with a unified skew-normal. Due to this, it is possible to study explicitly the posterior distribution along with the predictive probability mass function of the responses, and to derive a novel and more efficient sampler for high-dimensional inference. A conjugate class of priors for Bayesian probit regression, improving flexibility in prior specification without affecting tractability in posterior inference, is also provided.

Keywords: Bayesian Inference, Binary Data, Conjugacy, Probit Regression, Unified Skew-Normal.

1. Introduction

There is often a wide interest in many applied fields towards understanding how the probability mass function of a binary response variable $y \in \{0; 1\}$ changes with a set of predictors $\mathbf{x} = (x_1, \dots, x_p)^\top \in \mathbb{R}^p$ (e.g. Agresti, 2013). In addressing this goal, common models assume $\{y | \pi(\mathbf{x})\}$ is a Bernoulli variable $\{y | \pi(\mathbf{x})\} \sim \text{Bern}\{\pi(\mathbf{x})\}$, whose probability $\pi(\mathbf{x}) = \text{pr}(y = 1 | \mathbf{x}) \in (0, 1)$ is allowed to change with \mathbf{x} . Classical specifications for $\pi(\mathbf{x})$ are obtained by mapping a linear function $\eta(\mathbf{x}) = \sum_{j=1}^p x_j \beta_j = \mathbf{x}^\top \boldsymbol{\beta}$ of the predictors in the probability space via the probit or the logit link functions. In the first case $\pi(\mathbf{x}) = \Phi(\mathbf{x}^\top \boldsymbol{\beta})$ (e.g. Bliss, 1934, 1935), whereas in the second $\pi(\mathbf{x}) = \{1 + \exp(-\mathbf{x}^\top \boldsymbol{\beta})\}^{-1}$ (e.g. Dyke and Patterson, 1952; Cox, 1958), and the goal is provide inference on $\boldsymbol{\beta} = (\beta_1, \dots, \beta_p)^\top \in \mathbb{R}^p$.

Although frequentist inference for the above class of models is well-established (e.g. Agresti, 2013), the Bayesian approach has attracted an increasing interest due to the possibility of borrowing information, quantifying uncertainty, inducing automatic shrinkage and providing tractable inference via

the posterior distribution for the regression coefficients (e.g. Agresti, 2013, Chapter 7.2). Besides this, predictor-dependent models for binary data are also a fundamental building-block in more complex Bayesian formulations. Relevant examples include flexible nonparametric models for density regression (Leonard, 1978; Ren et al., 2011; Rodriguez and Dunson, 2011), neural networks (Jordan et al., 1999), additive regression trees (Chipman et al., 2010), graphical models (Spiegelhalter and Lauritzen, 1990), and hierarchical mixtures of experts (Jordan and Jacobs, 1994), among others. Although these methodologies provide fundamental learning procedures, there are still computational barriers which partially discourage a routine implementation. Indeed, differently from classical Bayesian regression for Gaussian responses, there are no results in the current literature for logit and probit models which allow analytical derivation of the posterior distribution for β , under the usual Gaussian prior.

Motivated by this apparent lack of conjugacy, a wide variety of computational methods for Bayesian logit and probit models have been developed. Popular routines consider data augmentation strategies which translate the logit or probit model for the original binary response data into a classical Bayesian linear regression for a set of latent Gaussian outcomes—within a Gibbs sampler. Notable contributions are the data augmentation via truncated Gaussians devised by Albert and Chib (1993) for the probit model, and the recent Pòlya-gamma data augmentation for logistic regression proposed by Polson et al. (2013); see also Holmes and Held (2006) and Frühwirth-Schnatter and Frühwirth (2007) for alternative proposals. Although these MCMC routines have been successfully applied in several contexts and have theoretical guarantees (Roy and Hobert, 2007; Choi and Hobert, 2013), there are still computational issues which deserve improved studies. In fact, besides the common bottlenecks of data augmentation MCMC in high dimensions, as discussed in Johndrow et al. (2017), these strategies provide a poor convergence and mixing in practice, especially for imbalanced data settings and for hierarchical models.

A possible alternative to partially overcome the above issues and scale-up computations is to rely on approximate inference in probit and logit regression via Laplace approximations (e.g. Spiegelhalter and Lauritzen, 1990; Chopin and Ridgway, 2017), variational Bayes (e.g. Jaakkola and Jordan, 2000; Consonni and Marin, 2007; Armagan and Zaretski, 2011) or expectation propagation (e.g. Chopin and Ridgway, 2017). Although such methods bypass some issues of data augmentation MCMC, these routines commonly provide a Gaussian approximation which could fundamentally affect the quality of inference and prediction when the posterior is skewed or has heavy tails. In fact, this behavior is common in many regression models for binary data (e.g. Kuss and Rasmussen, 2005; Rue et al., 2009). Possible solutions to this problem can be found in the integrated nested Laplace approximations (Rue et al., 2009) and in variational Bayes methods based on approximations via mixture models (Zobay, 2014). However, the increased flexibility of these methodologies comes at cost in terms of tractability. Moreover, such procedures are clearly still sub-optimal compared to situations in which the posterior distribution is analytically available and belongs to some well-known class of random variables.

This contribution proves that when the focus is on probit regression under a default Gaussian prior for the coefficients in β , the posterior is analytically available and coincides with the class of unified

skew-normal distributions (Arellano-Valle and Azzalini, 2006). Hence, although the aforementioned methods are still necessary for logit models, Bayesian inference under the probit link can potentially proceed via direct analysis of the unified skew-normal posterior. Note that the skew-normal has been already applied in probit regression to obtain a more flexible link function via skewed augmented data, instead of Gaussian ones (e.g. Chen et al., 1999; Bazán et al., 2006). This is clearly a fundamentally different focus than the one motivating this article.

To the best of the author's knowledge, exact posteriors for probit models are not currently available in the literature, but can provide fundamental advances in Bayesian binary regression and in more complex models exploiting such representation as a basic building-block. As discussed in the upcoming Sections, the availability of an exact posterior from a well-studied class of unified skew-normal distributions (Arellano-Valle and Azzalini, 2006; Gupta et al., 2013; Azzalini, 2013) overcomes the need of MCMC routines and approximate inference, especially in low-sample size problems, including large p and small n situations. Moreover, the exact posterior facilitates studies on finite-sample and asymptotic properties. For instance, in this case it is possible to formally study the sources of skewness and heavy tails currently found in several empirical studies. Finally, even when the main focus of inference is on high-dimensional sample size problems, a novel and efficient sampler—which relies on an additive representation of the unified skew-normal via a linear combination of p -variate Gaussians and n -variate truncated Gaussians—can be derived adapting recent Hamiltonian Monte Carlo (HMC) methods for multivariate truncated Gaussians (Pakman and Paninski, 2014). This novel sampler for unified skew-normals is useful beyond the Bayesian probit regression and can be applied more broadly to statistical models relying on high-dimensional unified skew-normal variables, thus overcoming the general issues associated with n -variate truncated Gaussians having large n .

The above results are described in Section 2; first for an illustrative case—see Section 2.1—and then for the general setting with y_1, \dots, y_n independent observations from a probit regression—see Section 2.2. A particular focus is paid to the derivation of the exact unified skew-normal posterior, along with its marginals, the associated posterior moments, and the analytical posterior predictive distribution induced on the binary responses. A novel efficient algorithm for high-dimensional problems, which applies recent HMC methods to a simple additive representation of the unified skew-normal, is provided in Section 2.2.2, and is compared with popular data augmentation MCMC for Bayesian probit regression (Albert and Chib, 1993) in Section 3. Motivated by these excellent results, a conjugate class of unified skew-normal priors for Bayesian probit regression is introduced in Section 2.2.4. This class crucially improves flexibility in prior specification—compared to default Gaussian settings—without affecting tractability in posterior inference. Concluding remarks can be found in Section 4.

2. Unified skew-normal posterior in Bayesian probit regression with Gaussian priors

Before deriving the skew-normal posterior induced by a Gaussian prior for the β coefficients in a probit regression, let us first introduce the unified skew-normal variables (SUN). Recalling Arellano-Valle and

Azzalini (2006) this very general class unifies different generalizations of the original multivariate skew-normal $\mathbf{z} \sim \text{SN}_p(\boldsymbol{\xi}, \boldsymbol{\Omega}, \boldsymbol{\alpha})$ (Azzalini and Dalla Valle, 1996) whose density $2\phi_p(\mathbf{z} - \boldsymbol{\xi}; \boldsymbol{\Omega})\Phi\{\boldsymbol{\alpha}^\top \boldsymbol{\omega}^{-1}(\mathbf{z} - \boldsymbol{\xi})\}$ is obtained by modifying the one of a p -variate Gaussian $\text{N}_p(\boldsymbol{\xi}, \boldsymbol{\Omega})$, with the cumulative distribution function of a $\text{N}(0, 1)$ evaluated at $\boldsymbol{\alpha}^\top \boldsymbol{\omega}^{-1}(\mathbf{z} - \boldsymbol{\xi})$, with $\boldsymbol{\omega} = \text{diag}(\Omega_{11}^{\frac{1}{2}}, \dots, \Omega_{pp}^{\frac{1}{2}})$. This approach effectively introduces a degree of skewness in $\text{N}_p(\boldsymbol{\xi}, \boldsymbol{\Omega})$ controlled by the vector of parameters $\boldsymbol{\alpha} = (\alpha_1, \dots, \alpha_p)^\top \in \mathbb{R}^p$, with $\boldsymbol{\xi} = (\xi_1, \dots, \xi_p)^\top \in \mathbb{R}^p$ and $\boldsymbol{\Omega}$ still driving location and variability, respectively (e.g. Arellano-Valle and Azzalini, 2006). Indeed, when $\boldsymbol{\alpha} = \mathbf{0}$ the multivariate skew-normal coincides with a Gaussian variable $\text{N}_p(\boldsymbol{\xi}, \boldsymbol{\Omega})$, whereas, setting $p = 1$ leads to the original univariate skew-normal $\text{SN}(\xi, \omega^2, \alpha)$ with density $2\phi(z - \xi; \omega^2)\Phi\{\alpha\omega^{-1}(z - \xi)\}$ (Azzalini, 1985).

Motivated by the success of the above basic formulations in different applied fields (e.g. Azzalini and Capitanio, 1999), several extensions have been proposed to incorporate additional relevant properties. Two important generalizations are obtained by adding an additional parameter $\boldsymbol{\gamma}$ in $\Phi\{\boldsymbol{\alpha}^\top \boldsymbol{\omega}^{-1}(\mathbf{z} - \boldsymbol{\xi})\}$ to develop a multivariate extended skew-normal distribution (Arnold and Beaver, 2000; Arnold et al., 2002), and by allowing also the truncation mechanism to be multivariate, thus providing the closed skew-normal family (Gupta et al., 2004; González-Farias et al., 2004). Besides increasing flexibility in characterizing skewness and heavy tails (e.g. Canale, 2011), such extensions allow closure properties for the marginals, conditionals and joint distributions, thus providing a very general class. Arellano-Valle and Azzalini (2006) unify the above generalizations within a single and tractable representation—namely the unified skew-normal distribution (SUN)—obtaining the following density function

$$\phi_p(\mathbf{z} - \boldsymbol{\xi}; \boldsymbol{\Omega}) \frac{\Phi_n\{\boldsymbol{\gamma} + \boldsymbol{\Delta}^\top \bar{\boldsymbol{\Omega}}^{-1} \boldsymbol{\omega}^{-1}(\mathbf{z} - \boldsymbol{\xi}); \boldsymbol{\Gamma} - \boldsymbol{\Delta}^\top \bar{\boldsymbol{\Omega}}^{-1} \boldsymbol{\Delta}\}}{\Phi_n(\boldsymbol{\gamma}; \boldsymbol{\Gamma})}, \quad (1)$$

for the random variable $\mathbf{z} \sim \text{SUN}_{p,n}(\boldsymbol{\xi}, \boldsymbol{\Omega}, \boldsymbol{\Delta}, \boldsymbol{\gamma}, \boldsymbol{\Gamma})$. In (1), $\phi_p(\mathbf{z} - \boldsymbol{\xi}; \boldsymbol{\Omega})$ is the density of a p -variate Gaussian with mean $\boldsymbol{\xi} = (\xi_1, \dots, \xi_p)^\top \in \mathbb{R}^p$ and $p \times p$ variance-covariance matrix $\boldsymbol{\Omega} = \boldsymbol{\omega} \bar{\boldsymbol{\Omega}} \boldsymbol{\omega}$, obtained via the quadratic combination between a correlation matrix $\bar{\boldsymbol{\Omega}}$ and a positive definite diagonal matrix $\boldsymbol{\omega} = \text{diag}(\Omega_{11}^{\frac{1}{2}}, \dots, \Omega_{pp}^{\frac{1}{2}})$. The quantities $\Phi_n\{\boldsymbol{\gamma} + \boldsymbol{\Delta}^\top \bar{\boldsymbol{\Omega}}^{-1} \boldsymbol{\omega}^{-1}(\mathbf{z} - \boldsymbol{\xi}); \boldsymbol{\Gamma} - \boldsymbol{\Delta}^\top \bar{\boldsymbol{\Omega}}^{-1} \boldsymbol{\Delta}\}$ and $\Phi_n(\boldsymbol{\gamma}; \boldsymbol{\Gamma})$ denote instead the cumulative distribution functions of the multivariate Gaussians $\text{N}_n(\mathbf{0}, \boldsymbol{\Gamma} - \boldsymbol{\Delta}^\top \bar{\boldsymbol{\Omega}}^{-1} \boldsymbol{\Delta})$ and $\text{N}_n(\mathbf{0}, \boldsymbol{\Gamma})$, evaluated at $\boldsymbol{\gamma} + \boldsymbol{\Delta}^\top \bar{\boldsymbol{\Omega}}^{-1} \boldsymbol{\omega}^{-1}(\mathbf{z} - \boldsymbol{\xi})$ and $\boldsymbol{\gamma}$, respectively. Similarly to the simpler multivariate skew-normal previously discussed, the $p \times n$ matrix $\boldsymbol{\Delta}$ has the main effect on skewness. In fact, when $\boldsymbol{\Delta}$ is zero, (1) coincides with the density of a $\text{N}_p(\boldsymbol{\xi}, \boldsymbol{\Omega})$. The vector $\boldsymbol{\gamma} \in \mathbb{R}^n$ adds additional flexibility in such departures from Gaussian assumptions, consistent with the multivariate extended skew-normal. Refer to Arellano-Valle and Azzalini (2006), Gupta et al. (2013) and Azzalini (2013, Chapter 7.1.2) for additional properties of the SUN.

Sections 2.1–2.2 prove that the posterior for the coefficients in a probit model with Gaussian priors is a SUN, and study the consequences of this novel finding in inference, prediction and computation.

2.1. An illustrative example with a single observation and a single covariate

To introduce the reader to the general situation consisting of y_1, \dots, y_n independent observations from a probit model with Gaussian prior $\pi(\boldsymbol{\beta}) = \phi_p(\boldsymbol{\beta} - \boldsymbol{\xi}; \boldsymbol{\Omega})$ for $\boldsymbol{\beta}$, let us first consider a simple case with a

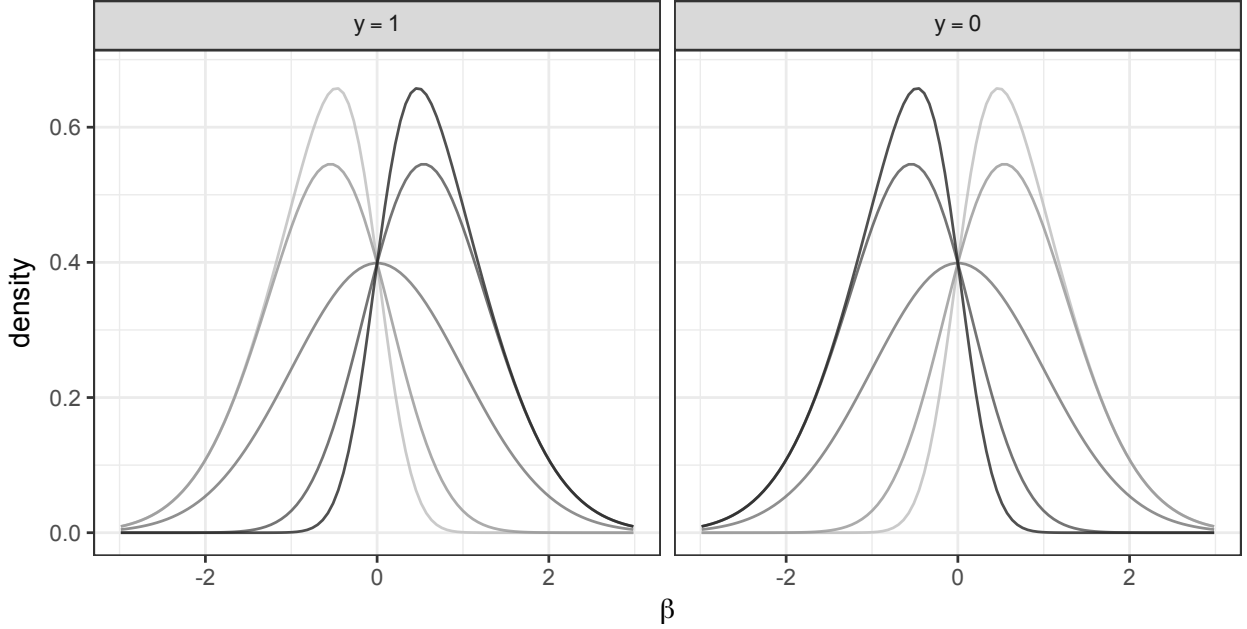


Fig. 1. Density of a $\text{SUN}_{1,1}\{0, 1, (2y - 1)x, 0, 1 + x^2\}$ posterior for β , for different combinations of x and y . The colors range from light grey to dark grey as $x \in (-3, -1.5, 0, 1.5, 3)$ goes from -3 to 3 .

single data point y from a probit model with only one covariate x —i.e. $(y | x, \beta) \sim \text{Bern}\{\Phi(x\beta)\}$ —and β having a standard Gaussian prior—i.e $\pi(\beta) = \phi(\beta; 1) = \phi(\beta)$. Although such scenario is uncommon in practical applications, it provides relevant intuitions on the role of the predictor x and the response y in driving departures from normality in the posterior distribution. Indeed, consistent with Lemma 1, $(\beta | y, x) \sim \text{SUN}_{1,1}\{0, 1, (2y - 1)x, 0, 1 + x^2\}$, when $\pi(\beta) = \phi(\beta)$.

LEMMA 1. *Let $(y | x, \beta) \sim \text{Bern}\{\Phi(x\beta)\}$ and $\pi(\beta) = \phi(\beta)$, then $(\beta | y, x) \sim \text{SUN}_{1,1}\{0, 1, (2y - 1)x, 0, 1 + x^2\}$ for every $x \in \mathbb{R}$ and $y \in \{0; 1\}$.*

PROOF. Let $P(y | x, \beta) = \Phi(x\beta)^y \{1 - \Phi(x\beta)\}^{1-y} = \Phi\{(2y - 1)x\beta\}$ denote the probability mass function of $(y | x, \beta) \sim \text{Bern}\{\Phi(x\beta)\}$. Direct application of the Bayes theorem provides $\pi(\beta | y, x) \propto \phi(\beta)\Phi\{(2y - 1)x\beta\}$. Therefore, letting $\gamma = 0$, $\Delta = (2y - 1)x$ and $\Gamma = 1 + \Delta^\top \Delta = 1 + x^2$, provides the kernel of a $\text{SUN}_{1,1}\{0, 1, (2y - 1)x, 0, 1 + x^2\}$, thus concluding the proof. It is interesting to note how the construction of the posterior is in the same spirit of the perturbation strategy outlined by Azzalini (2013, Chapter 1.3) to induce skewness in symmetric densities. In this case, the prior defines the original base density, whereas the likelihood induces the perturbation. \square

Figure 1 provides the density function of the SUN posterior for β in the simple illustrative example, considering different combinations of x and y . As expected, $\Delta = (2y - 1)x$ has a main role in inducing skewness. Indeed, the higher $|x|$ the more skewness is observed in the posterior $\pi(\beta | y, x)$. Such skewness is either positive or negative depending on the sign of $(2y - 1)x$. To better understand the role of x and y in the shape of the skew-normal posterior, note that a $\text{SUN}_{1,1}\{0, 1, (2y - 1)x, 0, 1 + x^2\}$

coincides indeed with a very simple $\text{SN}\{0, 1, (2y - 1)x\}$. In fact, $\pi(\beta \mid y, x) = 2\phi(\beta)\Phi\{(2y - 1)x\beta\}$. Based on this connection and on the results in Azzalini (2013, Chapter 2.1.4), it can be easily shown that $E(\beta \mid y, x) = \sqrt{2}(2y - 1)x\{\pi(1 + x^2)\}^{-\frac{1}{2}}$, $\text{var}(\beta \mid y, x) = 1 - 2x^2\{\pi(1 + x^2)\}^{-1}$, $\gamma_1(\beta \mid y, x) = (4 - \pi)(2y - 1)^3x^3\sqrt{2}\{\pi(1 + x^2) - 2x^2\}^{-\frac{3}{2}}$ and $\gamma_2(\beta \mid y, x) = 8(\pi - 3)x^4\{\pi(1 + x^2) - 2x^2\}^{-2}$, where $\gamma_1(\beta \mid y, x)$ and $\gamma_2(\beta \mid y, x)$ denote the usual indices of skewness and excess kurtosis, respectively.

Computing the above quantities for $y = 1$ and the combinations of $x \in (-3, -1.5, 0, 1.5, 3)$ in Figure 1, provides $(-0.76, -0.66, 0.00, 0.66, 0.76)$, $(0.43, 0.56, 1.00, 0.56, 0.43)$, $(-0.67, -0.30, 0.00, 0.30, 0.67)$, and $(0.51, 0.18, 0.00, 0.18, 0.51)$, for the expectation, variance, skewness and excess kurtosis, respectively. When $y = 0$, the variance and the excess kurtosis remain the same, whereas the expectation and skewness become $(0.76, 0.66, 0.00, -0.66, -0.76)$ and $(0.67, 0.30, 0.00, -0.30, -0.67)$, respectively. Hence, consistent with Figure 1, growing values of $|x|$ induce more evident departures from the normality of the prior, both in term of skewness and excess kurtosis, while favoring growing changes in the expectation and a reduction in the variance of the posterior. The response data $y \in \{0; 1\}$ have instead a role in determining the sign of the expectation and the type of skewness. More specifically, the skewness is either positive or negative depending on the sign of $(2y - 1)x$.

2.2. The general Bayesian probit regression

The results in Section 2.1 apply more in general to the case of independent responses $\mathbf{y} = (y_1, \dots, y_n)^\top$ from a probit regression model $(y_i \mid \mathbf{x}_i, \boldsymbol{\beta}) \sim \text{Bern}\{\Phi(\mathbf{x}_i^\top \boldsymbol{\beta})\}$, $i = 1, \dots, n$, where $\mathbf{x}_i = (x_{i1}, \dots, x_{ip})^\top \in \mathbb{R}^p$ denotes the vector of covariates for unit i and $\boldsymbol{\beta} = (\beta_1, \dots, \beta_p)^\top \in \mathbb{R}^p$ are the associated coefficients. Indeed, according to Theorem 1, when $\boldsymbol{\beta}$ has a multivariate Gaussian prior $\boldsymbol{\beta} \sim \text{N}_p(\boldsymbol{\xi}, \boldsymbol{\Omega})$, the posterior coincides with a unified skew-normal distribution $(\boldsymbol{\beta} \mid \mathbf{y}, \mathbf{X}) \sim \text{SUN}_{p,n}(\boldsymbol{\xi}, \boldsymbol{\Omega}, \bar{\boldsymbol{\Omega}}\boldsymbol{\omega}\mathbf{D}^\top, \mathbf{D}\boldsymbol{\xi}, \mathbf{I}_n + \mathbf{D}\boldsymbol{\Omega}\mathbf{D}^\top)$, where $\mathbf{D} = \text{diag}(2y_1 - 1, \dots, 2y_n - 1)\mathbf{X}$, with \mathbf{X} the $n \times p$ design matrix having rows \mathbf{x}_i^\top , $i = 1, \dots, n$.

THEOREM 1. *If $(y_i \mid \mathbf{x}_i, \boldsymbol{\beta}) \sim \text{Bern}\{\Phi(\mathbf{x}_i^\top \boldsymbol{\beta})\}$ independently for $i = 1, \dots, n$ and $\boldsymbol{\beta} \sim \text{N}_p(\boldsymbol{\xi}, \boldsymbol{\Omega})$, then*

$$(\boldsymbol{\beta} \mid \mathbf{y}, \mathbf{X}) \sim \text{SUN}_{p,n}(\boldsymbol{\xi}, \boldsymbol{\Omega}, \bar{\boldsymbol{\Omega}}\boldsymbol{\omega}\mathbf{D}^\top, \mathbf{D}\boldsymbol{\xi}, \mathbf{I}_n + \mathbf{D}\boldsymbol{\Omega}\mathbf{D}^\top), \quad (2)$$

for every $\mathbf{D} = \text{diag}(2y_1 - 1, \dots, 2y_n - 1)\mathbf{X} \in \mathbb{R}^{n \times p}$, $\boldsymbol{\xi} = (\xi_1, \dots, \xi_p)^\top \in \mathbb{R}^p$, and positive definite matrix $\boldsymbol{\Omega} = \boldsymbol{\omega}\bar{\boldsymbol{\Omega}}\boldsymbol{\omega}$, with $\bar{\boldsymbol{\Omega}}$ a correlation matrix and $\boldsymbol{\omega} = \text{diag}(\Omega_{11}^{\frac{1}{2}}, \dots, \Omega_{pp}^{\frac{1}{2}})$.

PROOF. Adapting the proof of Lemma 1 to this regression case, it is possible to write the joint probability mass function of the responses \mathbf{y} as $P(\mathbf{y} \mid \mathbf{X}, \boldsymbol{\beta}) = \prod_{i=1}^n \Phi\{(2y_i - 1)\mathbf{x}_i^\top \boldsymbol{\beta}\} = \Phi_n(\mathbf{D}\boldsymbol{\beta}; \mathbf{I}_n)$, with $\mathbf{D} = \text{diag}(2y_1 - 1, \dots, 2y_n - 1)\mathbf{X}$. Combining this likelihood for \mathbf{y} with the Gaussian prior for $\boldsymbol{\beta}$, provides $\pi(\boldsymbol{\beta} \mid \mathbf{y}, \mathbf{X}) \propto \phi_p(\boldsymbol{\beta} - \boldsymbol{\xi}; \boldsymbol{\Omega})\Phi_n(\mathbf{D}\boldsymbol{\beta}; \mathbf{I}_n) = \phi_p(\boldsymbol{\beta} - \boldsymbol{\xi}; \boldsymbol{\Omega})\Phi_n\{\mathbf{D}\boldsymbol{\xi} + \mathbf{D}(\boldsymbol{\beta} - \boldsymbol{\xi}); \mathbf{I}_n\}$. To establish the connection between this kernel and (1), note that $\mathbf{D}(\boldsymbol{\beta} - \boldsymbol{\xi}) = \mathbf{D}\boldsymbol{\omega}\bar{\boldsymbol{\Omega}}\bar{\boldsymbol{\Omega}}^{-1}\boldsymbol{\omega}^{-1}(\boldsymbol{\beta} - \boldsymbol{\xi})$. Therefore, letting $\boldsymbol{\gamma} = \mathbf{D}\boldsymbol{\xi}$, $\boldsymbol{\Delta} = \bar{\boldsymbol{\Omega}}\boldsymbol{\omega}\mathbf{D}^\top$ and $\boldsymbol{\Gamma} = \mathbf{I}_n + \boldsymbol{\Delta}^\top \bar{\boldsymbol{\Omega}}^{-1}\boldsymbol{\Delta} = \mathbf{I}_n + \mathbf{D}\boldsymbol{\omega}\bar{\boldsymbol{\Omega}}\bar{\boldsymbol{\Omega}}^{-1}\bar{\boldsymbol{\Omega}}\boldsymbol{\omega}\mathbf{D}^\top = \mathbf{I}_n + \mathbf{D}\boldsymbol{\Omega}\mathbf{D}^\top$, provides the kernel of a $\text{SUN}_{p,n}(\boldsymbol{\xi}, \boldsymbol{\Omega}, \bar{\boldsymbol{\Omega}}\boldsymbol{\omega}\mathbf{D}^\top, \mathbf{D}\boldsymbol{\xi}, \mathbf{I}_n + \mathbf{D}\boldsymbol{\Omega}\mathbf{D}^\top)$, concluding the proof. \square

Based on Theorem 1, the density function of the posterior, is therefore

$$\pi(\boldsymbol{\beta} | \mathbf{y}, \mathbf{X}) = \phi_p(\boldsymbol{\beta} - \boldsymbol{\xi}; \boldsymbol{\Omega}) \frac{\Phi_n(\mathbf{D}\boldsymbol{\beta}; \mathbf{I}_n)}{\Phi_n(\mathbf{D}\boldsymbol{\xi}; \mathbf{I}_n + \mathbf{D}\boldsymbol{\Omega}\mathbf{D}^\top)} = \phi_p(\boldsymbol{\beta} - \boldsymbol{\xi}; \boldsymbol{\Omega}) \frac{\prod_{i=1}^n \Phi\{(2y_i - 1)\mathbf{x}_i^\top \boldsymbol{\beta}\}}{\Phi_n(\mathbf{D}\boldsymbol{\xi}; \mathbf{I}_n + \mathbf{D}\boldsymbol{\Omega}\mathbf{D}^\top)}, \quad (3)$$

with $\Phi_n(\mathbf{D}\boldsymbol{\xi}; \mathbf{I}_n + \mathbf{D}\boldsymbol{\Omega}\mathbf{D}^\top)$ being the normalizing constant. To better highlight the role of the hyperparameters $\boldsymbol{\xi}$ and $\boldsymbol{\Omega}$, along with that of the data \mathbf{y} and \mathbf{X} , let us consider a constructive representation of the unified skew-normal posterior. In particular, adapting current results for the unified skew-normal distribution to the posterior in (2), it can be easily shown that $(\boldsymbol{\beta} | \mathbf{y}, \mathbf{X})$ has the additive representation in Proposition 1.

PROPOSITION 1. *If $(\boldsymbol{\beta} | \mathbf{y}, \mathbf{X}) \sim \text{SUN}_{p,n}(\boldsymbol{\xi}, \boldsymbol{\Omega}, \bar{\boldsymbol{\Omega}}\boldsymbol{\omega}\mathbf{D}^\top, \mathbf{D}\boldsymbol{\xi}, \mathbf{I}_n + \mathbf{D}\boldsymbol{\Omega}\mathbf{D}^\top)$, then*

$$(\boldsymbol{\beta} | \mathbf{y}, \mathbf{X}) = \boldsymbol{\xi} + \boldsymbol{\Omega}\{\mathbf{V}_0 + \mathbf{D}^\top(\mathbf{I}_n + \mathbf{D}\boldsymbol{\Omega}\mathbf{D}^\top)^{-1}\mathbf{V}_1\}, \quad (4)$$

with $\mathbf{V}_0 \sim \text{N}_p\{\mathbf{0}, \boldsymbol{\Omega}^{-1} - \mathbf{D}^\top(\mathbf{I}_n + \mathbf{D}\boldsymbol{\Omega}\mathbf{D}^\top)^{-1}\mathbf{D}\}$, and $\mathbf{V}_1 \sim \text{TN}_n(-\mathbf{D}\boldsymbol{\xi}; \mathbf{0}, \mathbf{I}_n + \mathbf{D}\boldsymbol{\Omega}\mathbf{D}^\top)$ from an n -variate Gaussian with mean $\mathbf{0}$, variance-covariance matrix $\mathbf{I}_n + \mathbf{D}\boldsymbol{\Omega}\mathbf{D}^\top$ and truncation below $-\mathbf{D}\boldsymbol{\xi}$. Moreover, $(\mathbf{I}_n + \mathbf{D}\boldsymbol{\Omega}\mathbf{D}^\top)^{-1} = \mathbf{I}_n - \mathbf{D}(\boldsymbol{\Omega}^{-1} + \mathbf{D}^\top\mathbf{D})^{-1}\mathbf{D}^\top$, thus allowing the computational complexity associated with the inversion of $\mathbf{I}_n + \mathbf{D}\boldsymbol{\Omega}\mathbf{D}^\top$ to depend on p , rather than on the sample size n .

PROOF. The proof is a simple adaptation of equation (7.4) in Azzalini (2013, Chapter 7.1.2) to the specific form of the posterior in (2). In particular, since $\boldsymbol{\Omega} = \boldsymbol{\omega}\bar{\boldsymbol{\Omega}}\boldsymbol{\omega}$, the additive representation in (4) can be also rewritten as $(\boldsymbol{\beta} | \mathbf{y}, \mathbf{X}) = \boldsymbol{\xi} + \boldsymbol{\omega}\{\bar{\boldsymbol{\Omega}}\boldsymbol{\omega}\mathbf{V}_0 + \bar{\boldsymbol{\Omega}}\boldsymbol{\omega}\mathbf{D}^\top(\mathbf{I}_n + \mathbf{D}\boldsymbol{\Omega}\mathbf{D}^\top)^{-1}\mathbf{V}_1\}$. Moreover, exploiting the standard properties of multivariate Gaussian variables, it can be easily shown that, if $\mathbf{V}_0 \sim \text{N}_p\{\mathbf{0}, \boldsymbol{\Omega}^{-1} - \mathbf{D}^\top(\mathbf{I}_n + \mathbf{D}\boldsymbol{\Omega}\mathbf{D}^\top)^{-1}\mathbf{D}\}$, then $\mathbf{U}_0 = \bar{\boldsymbol{\Omega}}\boldsymbol{\omega}\mathbf{V}_0 \sim \text{N}_p\{\mathbf{0}, \bar{\boldsymbol{\Omega}} - \bar{\boldsymbol{\Omega}}\boldsymbol{\omega}\mathbf{D}^\top(\mathbf{I}_n + \mathbf{D}\boldsymbol{\Omega}\mathbf{D}^\top)^{-1}\mathbf{D}\bar{\boldsymbol{\Omega}}\}$. Consistent with the proof of Theorem 1, $\boldsymbol{\gamma} = \mathbf{D}\boldsymbol{\xi}$, $\boldsymbol{\Delta} = \bar{\boldsymbol{\Omega}}\boldsymbol{\omega}\mathbf{D}^\top$ and $\boldsymbol{\Gamma} = \mathbf{I}_n + \mathbf{D}\boldsymbol{\Omega}\mathbf{D}^\top$. Therefore, making these substitutions, it is possible to write the additive representation as $\boldsymbol{\xi} + \boldsymbol{\omega}(\mathbf{U}_0 + \boldsymbol{\Delta}\boldsymbol{\Gamma}^{-1}\mathbf{U}_1)$, $\mathbf{U}_0 \sim \text{N}_p\{\mathbf{0}, \bar{\boldsymbol{\Omega}} - \boldsymbol{\Delta}\boldsymbol{\Gamma}^{-1}\boldsymbol{\Delta}^\top\}$ and $\mathbf{U}_1 \sim \text{TN}_n(-\boldsymbol{\gamma}; \mathbf{0}, \boldsymbol{\Gamma})$, thus obtaining the same representation provided by Azzalini (2013, Chapter 7.1.2) in equation (7.4) for a $\text{SUN}_{p,n}(\boldsymbol{\xi}, \boldsymbol{\Omega}, \boldsymbol{\Delta}, \boldsymbol{\gamma}, \boldsymbol{\Gamma})$. Note that, differently from Arellano-Valle and Azzalini (2006), Azzalini (2013, Chapter 7.1.2) denote the truncation parameter with $\boldsymbol{\tau}$, instead of $\boldsymbol{\gamma}$. The result $(\mathbf{I}_n + \mathbf{D}\boldsymbol{\Omega}\mathbf{D}^\top)^{-1} = \mathbf{I}_n - \mathbf{D}(\boldsymbol{\Omega}^{-1} + \mathbf{D}^\top\mathbf{D})^{-1}\mathbf{D}^\top$ is instead a simple application of the Woodbury identity. \square

Based on the additive representation (4), the prior mean $\boldsymbol{\xi}$ has a main role on the location of the posterior, but has also an effect in controlling departures from normality both in terms of skewness and excess kurtosis (e.g. Azzalini, 2013; Canale, 2011), since it appears in the truncation parameter $\boldsymbol{\gamma} = \mathbf{D}\boldsymbol{\xi}$. The prior variance-covariance matrix $\boldsymbol{\Omega}$ has mostly an effect on scale and posterior dependence among the $\boldsymbol{\beta}$ parameters, but contributes also to the shape of the posterior in controlling the weight assigned to the multivariate truncated Gaussians \mathbf{V}_1 , along with its variability. Finally, also the data in $\mathbf{D} = \text{diag}(2y_1 - 1, \dots, 2y_n - 1)\mathbf{X}$ play more than a role in term of location, scale and departures from normality. In particular, note that if the matrix \mathbf{D} has elements very close to $\mathbf{0}$, the multivariate truncated Gaussians \mathbf{V}_1 —which induces departures from normality in $(\boldsymbol{\beta} | \mathbf{y}, \mathbf{X})$ —has a negligible importance compared to the multivariate Gaussian \mathbf{V}_0 in the additive representation (4).

2.2.1. Closure properties of the SUN posterior

A fundamental property of the SUN, which potentially facilitates posterior inference, is that this class of variables is closed under marginalization and linear combinations (Arellano-Valle and Azzalini, 2006; Gupta et al., 2013; Azzalini, 2013). In particular, adapting the results in Arellano-Valle and Azzalini (2006) to the unified skew-normal in equation (2), the marginal posteriors $(\beta_j | \mathbf{y}, \mathbf{X})$, $j = 1, \dots, p$, still belong to the SUN family and coincide with $(\beta_j | \mathbf{y}, \mathbf{X}) \sim \text{SUN}_{1,n}(\xi_j, \omega_{jj}^2, \Delta_j, \mathbf{D}\xi, \mathbf{I}_n + \mathbf{D}\Omega\mathbf{D}^\top)$, where ξ_j is the j th element of ξ , $\omega_{jj}^2 = \Omega_{jj}$ denotes the entry $[jj]$ in Ω , and finally Δ_j represents the j th row of $\Delta = \bar{\Omega}\omega\mathbf{D}^\top$. Exploiting this result, the density of the marginal posterior is

$$\pi(\beta_j | \mathbf{y}, \mathbf{X}) = \phi(\beta_j - \xi_j; \omega_{jj}^2) \frac{\Phi_n\{\mathbf{D}\xi + \Delta_j^\top \omega_{jj}^{-1}(\beta_j - \xi_j); \mathbf{I}_n + \mathbf{D}\Omega\mathbf{D}^\top - \Delta_j^\top \Delta_j\}}{\Phi_n(\mathbf{D}\xi; \mathbf{I}_n + \mathbf{D}\Omega\mathbf{D}^\top)}, \quad j = 1, \dots, p. \quad (5)$$

The above representation holds more in general for any $\beta_{\mathcal{J}}$, with \mathcal{J} a subset of the index set $\{1, \dots, p\}$. In particular, recalling Arellano-Valle and Azzalini (2006), it can be easily shown that $(\beta_{\mathcal{J}} | \mathbf{y}, \mathbf{X}) \sim \text{SUN}_{|\mathcal{J}|,n}(\xi_{\mathcal{J}}, \Omega_{\mathcal{J}\mathcal{J}}, \Delta_{\mathcal{J}}, \mathbf{D}\xi, \mathbf{I}_n + \mathbf{D}\Omega\mathbf{D}^\top)$, where $\xi_{\mathcal{J}}$ is the vector containing the elements in ξ with indices in the set \mathcal{J} , $\Omega_{\mathcal{J}\mathcal{J}}$ denotes the $|\mathcal{J}| \times |\mathcal{J}|$ block of Ω corresponding to the indices in \mathcal{J} , and finally $\Delta_{\mathcal{J}}$ is the $|\mathcal{J}| \times n$ matrix containing those rows of $\Delta = \bar{\Omega}\omega\mathbf{D}^\top$ indexed by elements in \mathcal{J} .

Also linear combinations $\eta(\beta) = \mathbf{a} + \mathbf{A}^\top \beta$ —with \mathbf{a} a $q \times 1$ location vector and \mathbf{A} a full-rank $p \times q$ scale matrix—are often of interest in posterior inference. This is true, for instance, when the focus is on studying the posterior distribution of the linear predictor $\mathbf{x}^\top \beta$ for a given combination of covariates $\mathbf{x} = (x_1, \dots, x_p)^\top$. In this situation $a = 0$ and $\mathbf{A} = \mathbf{x}$. Adapting the closure properties of the SUN to the posterior in equation (2), also $\{\eta(\beta) | \mathbf{y}, \mathbf{X}\} \sim \text{SUN}_{q,n}(\mathbf{a} + \mathbf{A}^\top \xi, \mathbf{A}^\top \Omega \mathbf{A}, \Delta_{\mathbf{A}}, \mathbf{D}\xi, \mathbf{I}_n + \mathbf{D}\Omega\mathbf{D}^\top)$ with $\Delta_{\mathbf{A}} = \{(\mathbf{A}^\top \Omega \mathbf{A}) \odot \mathbf{I}_q\}^{-\frac{1}{2}} \mathbf{A}^\top \Omega \mathbf{D}^\top$, and \odot denoting the entry-wise or Hadamard product. Therefore, letting $\xi_{\mathbf{A}} = \mathbf{a} + \mathbf{A}^\top \xi$, $\omega_{\mathbf{A}} = \{(\mathbf{A}^\top \Omega \mathbf{A}) \odot \mathbf{I}_q\}^{\frac{1}{2}}$ and $\mathbf{A}^\top \Omega \mathbf{A} = \Omega_{\mathbf{A}} = \omega_{\mathbf{A}} \bar{\Omega}_{\mathbf{A}} \omega_{\mathbf{A}}$, the posterior density function of $\{\eta(\beta) | \mathbf{y}, \mathbf{X}\}$ is

$$\pi\{\eta(\beta) | \mathbf{y}, \mathbf{X}\} = \phi_q\{\eta(\beta) - \xi_{\mathbf{A}}; \Omega_{\mathbf{A}}\} \frac{\Phi_n\{\mathbf{D}\xi + \Delta_{\mathbf{A}}^\top \bar{\Omega}_{\mathbf{A}}^{-1} \omega_{\mathbf{A}}^{-1}(\eta(\beta) - \xi_{\mathbf{A}}); \mathbf{I}_n + \mathbf{D}\Omega\mathbf{D}^\top - \Delta_{\mathbf{A}}^\top \bar{\Omega}_{\mathbf{A}}^{-1} \Delta_{\mathbf{A}}\}}{\Phi_n(\mathbf{D}\xi; \mathbf{I}_n + \mathbf{D}\Omega\mathbf{D}^\top)}. \quad (6)$$

Although it is less common to provide posterior inference on the conditional posterior distribution $(\beta_{\mathcal{J}} | \mathbf{y}, \mathbf{X}, \beta_{\mathcal{J}^*})$ for a subset of coefficients $\beta_{\mathcal{J}}$, $\mathcal{J} \subset \{1, \dots, p\}$ given a set of others $\beta_{\mathcal{J}^*}$, $\mathcal{J}^* \subset \{1, \dots, p\}$ with $\mathcal{J} \cap \mathcal{J}^* = \emptyset$, it is worth noticing that the SUN is also closed under conditioning. Refer to Arellano-Valle and Azzalini (2006) and Azzalini (2013, Chapter 7.1.2) for details to obtain the SUN conditional posterior for $(\beta_{\mathcal{J}} | \mathbf{y}, \mathbf{X}, \beta_{\mathcal{J}^*})$ from the joint distribution in equation (2).

2.2.2. Posterior inference and computational aspects

Although posterior inference can proceed in many different directions, a general focus in Bayesian regression is on the marginal posteriors $(\beta_j | \mathbf{y}, \mathbf{X})$, $j = 1, \dots, p$, their associated moments—such as expectation, variance and skewness, among others—and more complex functionals including measures of posterior dependence and credible intervals or regions.

Leveraging the derivations in Section 2.2.1, the above goals can be easily addressed for each coefficient β_j , $j = 1, \dots, p$, and also for linear combinations $\eta(\beta) = \mathbf{a} + \mathbf{A}^\top \beta$ of the coefficients, whenever it is possible to evaluate $\phi(\cdot)$ and $\Phi_n(\cdot)$ with efficiency and accuracy. This is true for small sample-size studies—including popular large p and small n applications—and in statistical models admitting low-dimensional factorizations of $\Phi_n(\cdot)$. In these situations there exists a wide variety of procedures to evaluate $\Phi_n(\cdot)$ with precision and efficiency (Genz, 1992, 1993; Miwa et al., 2003; Mi et al., 2009), thus allowing direct graphical representation of the marginal posteriors and accurate calculation of univariate posterior functionals via simple one-dimensional numerical integration (e.g. Quarteroni et al. (2010, Chapter 9), Press et al. (2007, Chapter 4)). Such quadrature routines can be also considered to obtain credible intervals. It is also worth noticing that Gupta et al. (2013) recently obtained analytical expressions for the expectation and the variance-covariance matrix of a generic $\text{SUN}_{p,n}(\xi, \Omega, \Delta, \gamma, \Gamma)$ via direct derivation of the moment generating function—which is provided analytically in Arellano-Valle and Azzalini (2006); Gupta et al. (2013) and Azzalini (2013, Chapter 7.1.2). Indeed, adapting these results to the posterior in (2) a similar strategy can be considered when studying the functionals of the SUN posterior, provided that the moment generating function $M(\mathbf{t})$ of $(\beta | \mathbf{y}, \mathbf{X})$ is

$$M(\mathbf{t}) = \exp(\xi^\top \mathbf{t} + 0.5 \mathbf{t}^\top \Omega \mathbf{t}) \frac{\Phi_n(\mathbf{D}\xi + \mathbf{D}\Omega\mathbf{t}; \mathbf{I}_n + \mathbf{D}\Omega\mathbf{D}^\top)}{\Phi_n(\mathbf{D}\xi; \mathbf{I}_n + \mathbf{D}\Omega\mathbf{D}^\top)}, \quad \mathbf{t} \in \mathbb{R}^p. \quad (7)$$

Although it is possible to analytically compute the derivatives of $M(\mathbf{t})$ in (7) to obtain marginal and joint moments of the posterior, as noticed in Gupta et al. (2013), this procedure requires tedious and complicated calculations even for lower-order moments, and still needs repeated evaluation of $\Phi_n(\cdot)$.

In large n studies or when the interest is on higher-order functionals—including posterior measures of pairwise dependence, indices of multivariate skewness and credible regions—the above methods fall far short of the goal of providing tractable inference procedures. In fact, fast strategies to calculate $\Phi_n(\cdot)$ (Genz, 1992, 1993) are subject to errors which increase with n , thus introducing inaccuracies in (3) and (5). Moreover, although cubature methods for multidimensional integration (e.g. Quarteroni et al., 2010, Chapter 9.9) can be applied to the joint SUN posterior for subset of coefficients β_J , such routines are less efficient than quadrature algorithms, especially when the dimensions of the integrals are very large (e.g. Press et al., 2007, Chapter 4.8). In these situations, sampling from the posterior provides a tractable strategy—commonly adopted in the Bayesian framework—to obtain a graphical representation of its marginals and a numerical evaluation of generic functionals $g(\cdot)$ via Monte Carlo integration approximating $\bar{g}(\beta) = \int_{\mathcal{B}} g(\beta) \pi(\beta | \mathbf{y}, \mathbf{X}) d\beta$. Indeed, the availability of a large number of S replicates $\beta^{(1)}, \dots, \beta^{(S)}$ from the SUN posterior $(\beta | \mathbf{y}, \mathbf{X})$, allows accurate approximation of $\bar{g}(\beta)$ via $\sum_{s=1}^S g(\beta^{(s)})/S$, while facilitating graphical representation of marginal and joint posteriors.

Popular routines addressing the above goal require data augmentation MCMC (e.g. Albert and Chib, 1993; Holmes and Held, 2006; Frühwirth-Schnatter and Frühwirth, 2007; Polson et al., 2013), which can provide poor mixing and convergence, especially in imbalanced studies and in hierarchical models (Johndrow et al., 2017). This issue can be effectively addressed via the novel sampler in Algorithm 1, combining the additive representation (4) of the SUN posterior (2) with a recent HMC for multivariate

Algorithm 1: Steps of the HMC to sample from the sun posterior in (2)

begin

- [1] Sample $\mathbf{V}_0^{(1)}, \dots, \mathbf{V}_0^{(S)}$ independently from a Gaussian $N_p\{\mathbf{0}, \boldsymbol{\Omega}^{-1} - \mathbf{D}^\top(\mathbf{I}_n + \mathbf{D}\boldsymbol{\Omega}\mathbf{D}^\top)^{-1}\mathbf{D}\}$.
- [2] Sample $\mathbf{V}_1^{(1)}, \dots, \mathbf{V}_1^{(S)}$ from a multivariate truncated Gaussians $TN_n(-\mathbf{D}\boldsymbol{\xi}; \mathbf{0}, \mathbf{I}_n + \mathbf{D}\boldsymbol{\Omega}\mathbf{D}^\top)$. To do this let \mathbf{W} denote the n -variate Gaussian $N_n(\mathbf{0}, \mathbf{I}_n + \mathbf{D}\boldsymbol{\Omega}\mathbf{D}^\top)$ whose truncation below $-\mathbf{D}\boldsymbol{\xi}$ generates the multivariate truncated Gaussian $TN_n(-\mathbf{D}\boldsymbol{\xi}; \mathbf{0}, \mathbf{I}_n + \mathbf{D}\boldsymbol{\Omega}\mathbf{D}^\top)$. Under this representation, the HMC in Pakman and Paninski (2014)—available in the R library `tmg`—can be directly applied after letting $\mathbf{M} = (\mathbf{I}_n + \mathbf{D}\boldsymbol{\Omega}\mathbf{D}^\top)^{-1}$, $\mathbf{r} = \mathbf{0}$ and $Q(\mathbf{W}) = \mathbf{W} + \mathbf{D}\boldsymbol{\xi} \geq 0$ in their equations (1.1) and (1.2).
- [3] Compute $\boldsymbol{\beta}^{(1)}, \dots, \boldsymbol{\beta}^{(S)}$, via $\boldsymbol{\beta}^{(s)} = \boldsymbol{\xi} + \boldsymbol{\Omega}\{\mathbf{V}_0^{(s)} + \mathbf{D}^\top(\mathbf{I}_n + \mathbf{D}\boldsymbol{\Omega}\mathbf{D}^\top)^{-1}\mathbf{V}_1^{(s)}\}$ for each $s = 1, \dots, S$.

truncated Gaussian variables (Pakman and Paninski, 2014). Indeed, leveraging Proposition 1, sampling a value $\boldsymbol{\beta}^{(s)}$ from $(\boldsymbol{\beta} | \mathbf{y}, \mathbf{X})$, requires generating data $\mathbf{V}_0^{(s)} \sim N_p\{\mathbf{0}, \boldsymbol{\Omega}^{-1} - \mathbf{D}^\top(\mathbf{I}_n + \mathbf{D}\boldsymbol{\Omega}\mathbf{D}^\top)^{-1}\mathbf{D}\}$, $\mathbf{V}_1^{(s)} \sim TN_n(-\mathbf{D}\boldsymbol{\xi}; \mathbf{0}, \mathbf{I}_n + \mathbf{D}\boldsymbol{\Omega}\mathbf{D}^\top)$, and then calculating the linear combination of these values, outlined in equation (4). The two main computational bottlenecks in this routine are the inversion of the $n \times n$ matrix $\mathbf{I}_n + \mathbf{D}\boldsymbol{\Omega}\mathbf{D}^\top$, and the sampling from the n -variate truncated Gaussian \mathbf{V}_1 . The first issue can be easily addressed exploiting the results in Proposition 1, which allow the computational complexity associated with the inversion of $\mathbf{I}_n + \mathbf{D}\boldsymbol{\Omega}\mathbf{D}^\top$ to depend on the number of covariates p , rather than on the sample size n —provided that $(\mathbf{I}_n + \mathbf{D}\boldsymbol{\Omega}\mathbf{D}^\top)^{-1} = \mathbf{I}_n - \mathbf{D}(\boldsymbol{\Omega}^{-1} + \mathbf{D}^\top\mathbf{D})^{-1}\mathbf{D}^\top$. Efficient sampling from \mathbf{V}_1 is instead less straightforward. Although classical rejection sampling from a multivariate truncated Gaussian is a simple possibility which provides an independent sampler (e.g. Wilhelm and Manjunath, 2010), such procedure has very low acceptance probability when n is large. A more practical solution is to leverage the closure properties of the multivariate truncated Gaussian under full conditioning (e.g. Kotecha and Djuric, 1999; Horrace, 2005), and sample iteratively each $V_{i1}^{(s)}$, $i = 1, \dots, n$ conditioned on the most recent values of the other entries comprising the $(n-1) \times 1$ vector $\mathbf{V}_{-i1}^{(s)}$. This leads to a simple Gibbs sampler (Kotecha and Djuric, 1999) which has been also implemented in the R library `tmvtnorm` (e.g. Wilhelm and Manjunath, 2010). Unfortunately, this routine inherits the same mixing issues of the data augmentation MCMC routines previously discussed.

To address the above issue, Algorithm 1 replaces the MCMC Gibbs sampler with a recent exact HMC for multivariate truncated Gaussians (Pakman and Paninski, 2014), available in the R library `tmg`. Although this strategy could still induce autocorrelation across samples, according to the empirical studies in Section 3, the mixing and the convergence performance of this routine is comparable to the one of an independent sampler, and massively improves current data augmentation MCMC methods, especially in imbalanced data sets. It is also worth noticing that Pakman and Paninski (2014) applied their HMC to Bayesian probit regression in an example relying on the augmented data representation devised by Albert and Chib (1993). Also this sampling mechanism provides major improvements in mixing and convergence, however, differently from Algorithm 1, the HMC proposed by Pakman and Paninski (2014) for Bayesian probit regression generates samples from an $n+p$ multivariate Gaussian

under linear inequalities—instead of allowing separate sampling from a p -variate Gaussian and an n -variate truncated Gaussian. Separating these two samplings, as in Algorithm 1, provides substantial improvements in computational tractability when p and n are large, while allowing parallel computing.

Before focusing on prediction, it is also worth emphasizing that Algorithm 1 provides a very general computational procedure to sample efficiently from a generic SUN random variable. This can be useful more broadly for any statistical model relying on high-dimensional unified skew-normal distributions, well beyond posterior inference in Bayesian probit regression. To the best of the author's knowledge, efficient samplers for the class of SUN random variables are still not available in the literature.

2.2.3. Prediction

Although inference on the posterior distribution of the regression coefficients $\beta \in \mathbb{R}^p$ is often of main interest, the prediction of a future binary response $y_{\text{new}} \in \{0; 1\}$ conditioned on the associated vector of covariates $\mathbf{x}_{\text{new}} \in \mathbb{R}^p$ and the current data (\mathbf{y}, \mathbf{X}) , is a primary goal in applications of Bayesian probit regression to classification problems and machine learning. Within a Bayesian framework, this requires the derivation of the posterior predictive distribution $(y_{\text{new}} | \mathbf{y}, \mathbf{X}, \mathbf{x}_{\text{new}})$, which in a binary case coincides with $\text{pr}(y_{\text{new}} = 1 | \mathbf{y}, \mathbf{X}, \mathbf{x}_{\text{new}}) = 1 - \text{pr}(y_{\text{new}} = 0 | \mathbf{y}, \mathbf{X}, \mathbf{x}_{\text{new}}) = \int_{\mathcal{B}} \Phi(\mathbf{x}_{\text{new}}^\top \beta) \pi(\beta | \mathbf{y}, \mathbf{X}) d\beta$. According to Corollary 1, this quantity is available in explicit form, thus allowing simple prediction without the need of sampling from $(\beta | \mathbf{y}, \mathbf{X})$.

COROLLARY 1. *If $(y_i | \mathbf{x}_i, \beta) \sim \text{Bern}\{\Phi(\mathbf{x}_i^\top \beta)\}$, for $i = 1, \dots, n$, and $\beta \sim N_p(\xi, \Omega)$, then*

$$\text{pr}(y_{\text{new}} = 1 | \mathbf{y}, \mathbf{X}, \mathbf{x}_{\text{new}}) = 1 - \text{pr}(y_{\text{new}} = 0 | \mathbf{y}, \mathbf{X}, \mathbf{x}_{\text{new}}) = \frac{\Phi_{n+1}(\mathbf{D}_{\text{new}} \xi; \mathbf{I}_{n+1} + \mathbf{D}_{\text{new}} \Omega \mathbf{D}_{\text{new}}^\top)}{\Phi_n(\mathbf{D} \xi; \mathbf{I}_n + \mathbf{D} \Omega \mathbf{D}^\top)}, \quad (8)$$

with \mathbf{D}_{new} denoting the $(n+1) \times p$ matrix obtained by adding a last row $\mathbf{x}_{\text{new}}^\top$ to \mathbf{D} .

PROOF. Recalling the results in Section 2.2, the posterior predictive probability $\text{pr}(y_{\text{new}} = 1 | \mathbf{y}, \mathbf{X}, \mathbf{x}_{\text{new}}) = \int_{\mathcal{B}} \Phi(\mathbf{x}_{\text{new}}^\top \beta) \pi(\beta | \mathbf{y}, \mathbf{X}) d\beta$ can be expressed as $\text{pr}(y_{\text{new}} = 1 | \mathbf{y}, \mathbf{X}, \mathbf{x}_{\text{new}}) = \Phi_n(\mathbf{D} \xi; \mathbf{I}_n + \mathbf{D} \Omega \mathbf{D}^\top)^{-1} \int_{\mathcal{B}} \phi_p(\beta - \xi; \Omega) \Phi(\mathbf{x}_{\text{new}}^\top \beta) \Phi_n(\mathbf{D} \beta; \mathbf{I}_n) d\beta$. Letting \mathbf{D}_{new} be the $(n+1) \times p$ matrix obtained by adding a last row $\mathbf{x}_{\text{new}}^\top$ to $\mathbf{D} = \text{diag}(2y_1 - 1, \dots, 2y_n - 1) \mathbf{X}$, the quantity $\Phi(\mathbf{x}_{\text{new}}^\top \beta) \Phi_n(\mathbf{D} \beta; \mathbf{I}_n)$ in the integral can be re-written as $\Phi_{n+1}(\mathbf{D}_{\text{new}} \beta; \mathbf{I}_{n+1}) = \Phi_{n+1}\{\mathbf{D}_{\text{new}} \xi + \mathbf{D}_{\text{new}}(\beta - \xi); \mathbf{I}_{n+1}\}$. Hence, adapting the proof of Theorem 1 to this case, it can be easily noticed that $\phi_p(\beta - \xi; \Omega) \Phi(\mathbf{x}_{\text{new}}^\top \beta) \Phi_n(\mathbf{D} \beta; \mathbf{I}_n) = \phi_p(\beta - \xi; \Omega) \Phi_{n+1}\{\mathbf{D}_{\text{new}} \xi + \mathbf{D}_{\text{new}}(\beta - \xi); \mathbf{I}_{n+1}\}$ is the kernel of a SUN _{$p, n+1$} ($\xi, \Omega, \bar{\Omega} \omega \mathbf{D}_{\text{new}}^\top, \mathbf{D}_{\text{new}} \xi, \mathbf{I}_{n+1} + \mathbf{D}_{\text{new}} \Omega \mathbf{D}_{\text{new}}^\top$), with normalizing constant $\int_{\mathcal{B}} \phi_p(\beta - \xi; \Omega) \Phi_{n+1}(\mathbf{D}_{\text{new}} \beta; \mathbf{I}_{n+1}) d\beta = \Phi_{n+1}(\mathbf{D}_{\text{new}} \xi; \mathbf{I}_{n+1} + \mathbf{D}_{\text{new}} \Omega \mathbf{D}_{\text{new}}^\top)$. Therefore, $\text{pr}(y_{\text{new}} = 1 | \mathbf{y}, \mathbf{X}, \mathbf{x}_{\text{new}}) = \Phi_n(\mathbf{D} \xi; \mathbf{I}_n + \mathbf{D} \Omega \mathbf{D}^\top)^{-1} \Phi_{n+1}(\mathbf{D}_{\text{new}} \xi; \mathbf{I}_{n+1} + \mathbf{D}_{\text{new}} \Omega \mathbf{D}_{\text{new}}^\top)$, concluding the proof. \square

According to Corollary 1, the posterior predictive probability of the event $y_{\text{new}} = 1$ in a Bayesian probit regression with a Gaussian prior is available in analytic form and coincides with $\text{pr}(y_{\text{new}} = 1 | \mathbf{y}, \mathbf{X}, \mathbf{x}_{\text{new}}) = \Phi_n(\mathbf{D} \xi; \mathbf{I}_n + \mathbf{D} \Omega \mathbf{D}^\top)^{-1} \Phi_{n+1}(\mathbf{D}_{\text{new}} \xi; \mathbf{I}_{n+1} + \mathbf{D}_{\text{new}} \Omega \mathbf{D}_{\text{new}}^\top)$. The event $y_{\text{new}} = 0$ has instead posterior predictive probability $\text{pr}(y_{\text{new}} = 0 | \mathbf{y}, \mathbf{X}, \mathbf{x}_{\text{new}}) = \Phi_n(\mathbf{D} \xi; \mathbf{I}_n + \mathbf{D} \Omega \mathbf{D}^\top)^{-1} \{\Phi_n(\mathbf{D} \xi; \mathbf{I}_n + \mathbf{D} \Omega \mathbf{D}^\top)^{-1} \Phi_{n+1}(\mathbf{D}_{\text{new}} \xi; \mathbf{I}_{n+1} + \mathbf{D}_{\text{new}} \Omega \mathbf{D}_{\text{new}}^\top)\}$.

$\mathbf{D}\Omega\mathbf{D}^\top) - \Phi_{n+1}(\mathbf{D}_{\text{new}}\boldsymbol{\xi}; \mathbf{I}_{n+1} + \mathbf{D}_{\text{new}}\Omega\mathbf{D}_{\text{new}}^\top)\}$. A major benefit of these results—compared to current data augmentation MCMC routines for Bayesian binary regression (e.g. Albert and Chib, 1993; Holmes and Held, 2006; Frühwirth-Schnatter and Frühwirth, 2007; Polson et al., 2013)—is that prediction does not require Monte Carlo integration for $\int_{\boldsymbol{\beta}} \Phi(\mathbf{x}_{\text{new}}^\top \boldsymbol{\beta}) \pi(\boldsymbol{\beta} | \mathbf{y}, \mathbf{X}) d\boldsymbol{\beta}$ via sampling of the coefficients $\boldsymbol{\beta}$ from the posterior distribution. However, although (8) marginalizes out $\boldsymbol{\beta}$ analytically, some computational issues may still remain in the calculation of $\Phi_{n+1}(\cdot)$ and $\Phi_n(\cdot)$. Indeed, as already discussed in Section 2.2.2, tractable and fast computational strategies to evaluate the cumulative distribution function of a multivariate Gaussian rely on quasi-randomized Monte-Carlo methods (Genz, 1992, 1993) which can be unstable for large n . However, differently from the densities in (5) and the functionals associated with such densities, $\Phi_{n+1}(\cdot)$ and $\Phi_n(\cdot)$ in equation (8) do not depend on $\boldsymbol{\beta}$ and therefore need to be evaluated only once to obtain the posterior predictive probability mass function for y_{new} . Hence, a possible strategy to reduce the instability of the quasi-randomized Monte-Carlo methods for $\Phi_{n+1}(\cdot)$ and $\Phi_n(\cdot)$, is to evaluate the two quantities in (8) multiple times and then obtain the posterior predictive probability mass function based on the average of the different evaluations. Although being more on the practical side, as outlined in Section 3, this procedure is highly effective and bypass MCMC when the focus is only on prediction.

2.2.4. A general conjugate class for Bayesian probit regression

The derivations in Section 2.2 suggest the more general result outlined in Corollary 2, thereby allowing tractable inference in Bayesian probit regression under a wide variety of shapes for the prior of $\boldsymbol{\beta}$.

COROLLARY 2. *If $(y_i | \mathbf{x}_i, \boldsymbol{\beta}) \sim \text{Bern}\{\Phi(\mathbf{x}_i^\top \boldsymbol{\beta})\}$ independently for $i = 1, \dots, n$, and $\boldsymbol{\beta}$ is assigned a $\text{SUN}_{p,m}(\boldsymbol{\xi}, \boldsymbol{\Omega}, \boldsymbol{\Psi}, \boldsymbol{\tau}, \boldsymbol{\Lambda})$ prior, with $\boldsymbol{\Psi} \in \mathbb{R}^{p \times m}$, $\boldsymbol{\tau} \in \mathbb{R}^m$ and $\boldsymbol{\Lambda}$ a positive definite $m \times m$ matrix, then*

$$(\boldsymbol{\beta} | \mathbf{y}, \mathbf{X}) \sim \text{SUN}_{p,m+n}\{\boldsymbol{\xi}, \boldsymbol{\Omega}, (\boldsymbol{\Psi}, \bar{\boldsymbol{\Omega}}\boldsymbol{\omega}\mathbf{D}^\top), (\boldsymbol{\tau}^\top, \boldsymbol{\xi}^\top\mathbf{D}^\top)^\top, \boldsymbol{\Gamma}\}, \quad \text{with } \boldsymbol{\Gamma} = \begin{bmatrix} \boldsymbol{\Lambda} & \boldsymbol{\Psi}^\top\boldsymbol{\omega}\mathbf{D}^\top \\ \mathbf{D}\boldsymbol{\omega}\boldsymbol{\Psi} & \mathbf{I}_n + \mathbf{D}\boldsymbol{\Omega}\mathbf{D}^\top \end{bmatrix}, \quad (9)$$

for every $\mathbf{D} = \text{diag}(2y_1 - 1, \dots, 2y_n - 1)\mathbf{X} \in \mathbb{R}^{n \times p}$, $\boldsymbol{\xi} = (\xi_1, \dots, \xi_p)^\top \in \mathbb{R}^p$, and positive definite matrix $\boldsymbol{\Omega} = \boldsymbol{\omega}\bar{\boldsymbol{\Omega}}\boldsymbol{\omega}$, with $\bar{\boldsymbol{\Omega}}$ a correlation matrix and $\boldsymbol{\omega} = \text{diag}(\Omega_{11}^{\frac{1}{2}}, \dots, \Omega_{pp}^{\frac{1}{2}})$.

PROOF. To prove Corollary 2 it suffices to generalize results in Theorem 1. In particular, adapting the derivations in the proof of Theorem 1 to the case in which $\boldsymbol{\beta}$ has a $\text{SUN}_{p,m}(\boldsymbol{\xi}, \boldsymbol{\Omega}, \boldsymbol{\Psi}, \boldsymbol{\tau}, \boldsymbol{\Lambda})$ prior—instead of $\boldsymbol{\beta} \sim \text{N}_p(\boldsymbol{\xi}, \boldsymbol{\Omega})$ —provides $\pi(\boldsymbol{\beta} | \mathbf{y}, \mathbf{X}) \propto \phi_p(\boldsymbol{\beta} - \boldsymbol{\xi}, \boldsymbol{\Omega}) \Phi_n(\mathbf{D}\boldsymbol{\beta}; \mathbf{I}_n) \Phi_m\{\boldsymbol{\tau} + \boldsymbol{\Psi}^\top\bar{\boldsymbol{\Omega}}^{-1}\boldsymbol{\omega}^{-1}(\boldsymbol{\beta} - \boldsymbol{\xi}); \boldsymbol{\Lambda} - \boldsymbol{\Psi}^\top\bar{\boldsymbol{\Omega}}^{-1}\boldsymbol{\Psi}\}$. Recalling the proof of Theorem 1, the quantity $\Phi_n(\mathbf{D}\boldsymbol{\beta}; \mathbf{I}_n)$ can be re-written as $\Phi_n\{\mathbf{D}\boldsymbol{\xi} + (\bar{\boldsymbol{\Omega}}\boldsymbol{\omega}\mathbf{D}^\top)^\top\bar{\boldsymbol{\Omega}}^{-1}\boldsymbol{\omega}^{-1}(\boldsymbol{\beta} - \boldsymbol{\xi}); \mathbf{I}_n + \mathbf{D}\boldsymbol{\Omega}\mathbf{D}^\top - \mathbf{D}\boldsymbol{\omega}\bar{\boldsymbol{\Omega}}\bar{\boldsymbol{\Omega}}^{-1}\bar{\boldsymbol{\Omega}}\boldsymbol{\omega}\mathbf{D}^\top\}$. Consistent with this expression, let $\boldsymbol{\gamma} = (\boldsymbol{\tau}^\top, \boldsymbol{\xi}^\top\mathbf{D}^\top)^\top \in \mathbb{R}^{(m+n)}$, $\boldsymbol{\Delta} = (\boldsymbol{\Psi}, \bar{\boldsymbol{\Omega}}\boldsymbol{\omega}\mathbf{D}^\top) \in \mathbb{R}^{p \times (m+n)}$, and denote with $\boldsymbol{\Gamma}$ the $(m+n) \times (m+n)$ block matrix, having $\boldsymbol{\Gamma}_{[11]} = \boldsymbol{\Lambda}$, $\boldsymbol{\Gamma}_{[22]} = \mathbf{I}_n + \mathbf{D}\boldsymbol{\Omega}\mathbf{D}^\top$ and $\boldsymbol{\Gamma}_{[21]} = \boldsymbol{\Gamma}_{[12]}^\top = \mathbf{D}\boldsymbol{\omega}\boldsymbol{\Psi}$. According to these settings, the kernel of the posterior $\pi(\boldsymbol{\beta} | \mathbf{y}, \mathbf{X})$ can be expressed as $\phi_p(\boldsymbol{\beta} - \boldsymbol{\xi}, \boldsymbol{\Omega}) \Phi_{m+n}\{\boldsymbol{\gamma} + \boldsymbol{\Delta}^\top\bar{\boldsymbol{\Omega}}^{-1}\boldsymbol{\omega}^{-1}(\boldsymbol{\beta} - \boldsymbol{\xi}); \boldsymbol{\Gamma} - \boldsymbol{\Delta}^\top\bar{\boldsymbol{\Omega}}^{-1}\boldsymbol{\Delta}\}$, thus highlighting the kernel of the $\text{SUN}_{p,m+n}\{\boldsymbol{\xi}, \boldsymbol{\Omega}, (\boldsymbol{\Psi}, \bar{\boldsymbol{\Omega}}\boldsymbol{\omega}\mathbf{D}^\top), (\boldsymbol{\tau}^\top, \boldsymbol{\xi}^\top\mathbf{D}^\top)^\top, \boldsymbol{\Gamma}\}$ posterior in Corollary 2. \square

According to Corollary 2, tractable inference and prediction in Bayesian probit regression is possible for a broader class of priors beyond the multivariate Gaussian assumption. Indeed, all the results and methods discussed in Sections 2.2–2.2.3 can be directly generalized to this more general case, provided that the posterior in equation (9) belongs to the same class of the SUN in (2). This allows increased flexibility in prior specification, thus allowing departures from the normality assumption in terms of skewness and heavy tails. Although a fully general unified skew-normal $\text{SUN}_{p,m}(\boldsymbol{\xi}, \boldsymbol{\Omega}, \boldsymbol{\Psi}, \boldsymbol{\tau}, \boldsymbol{\Lambda})$ prior may not be a common choice in applied contexts, it shall be noticed that the SUN incorporates several priors of interest, including multivariate Gaussians, independent skew-normals or extended skew-normals for each β_1, \dots, β_p , and multivariate skew-normals or multivariate extended skew-normals for $\boldsymbol{\beta}$ (Arellano-Valle and Azzalini, 2006).

3. Empirical studies

To evaluate the analytical results and the algorithms presented in Section 2, while comparing such methods with popular strategies for Bayesian inference in probit regression models (Albert and Chib, 1993), let us consider different empirical studies, covering both simulations and real–data applications. In particular, Section 3.1 considers a simple illustrative simulation which highlights issues associated with popular data augmentation MCMC even in simplistic settings, and allows confirmative checks for the results and the analytical derivations in Section 2. Section 3.2 studies, instead, the extent at which the methods and the algorithms presented in Section 2 improve performance in posterior inference and prediction with a focus on two real–data applications from biostatistics, including a study having large p and small n .

3.1. Illustrative simulation study

Recalling Section 2.1, let us consider a simplistic scenario with a single observation $y = 1$ generated from an intercept–only Bayesian probit with success probability $\Phi(\beta) \in (0, 1)$ and prior $\beta \sim N(0, 100)$. Adapting the derivations in Section 2 to this simple setting, the posterior has density function $\pi(\beta | y = 1) = 2\phi(\beta; 100)\Phi(\beta)$, thus coinciding with a skew-normal $\text{SN}(0, 100, 1)$. Based on this analytical result, the density of $(\beta | y = 1)$ can be easily evaluated, thus allowing direct graphical visualization—see Figure 2—and simple calculation of relevant functionals via quadrature—see Table 1.

Although the above inference, which relies on the novel findings presented in this article, bypasses the need to sample from $(\beta | y = 1)$, let us compare the quantities obtained under the above analytical calculations with those provided by sampling methods. This additional assessment is useful to compare the performance of the HMC in Algorithm 1 with the more popular data augmentation MCMC routine in Albert and Chib (1993), and to obtain reassurance for the correctness and the efficiency of the routine developed, via comparison with analytical results. To accomplish this, both the data augmentation MCMC by Albert and Chib (1993)—implemented in the R library `bayesm`—and the HMC in Algorithm 1 were run for 10000 iterations after taking a burn–in of 5000. Although the HMC based on the additive

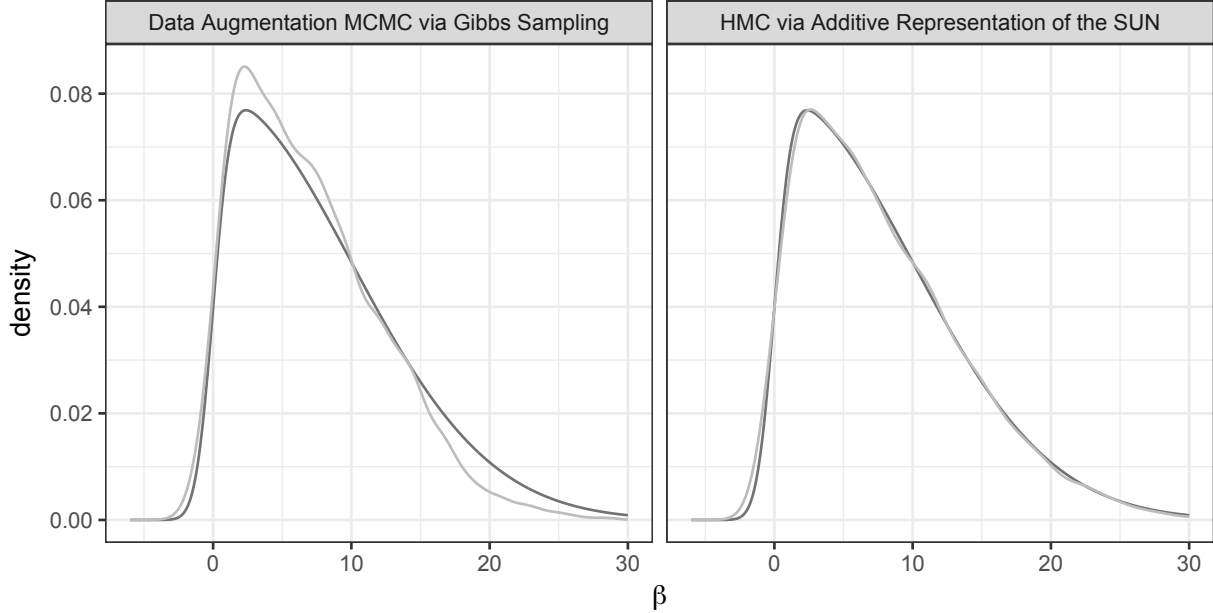


Fig. 2. Comparison between the exact posterior density of $(\beta | y = 1) \sim \text{SN}(0, 100, 1)$ (dark grey) and those obtained via a kernel density estimator (light grey) applied to the posterior samples from $(\beta | y = 1)$ generated by the data augmentation Gibbs sampler in Albert and Chib (1993) (left), and the HMC in Algorithm 1 (right), which relies on the additive representation of the SUN posterior.

Table 1. Expectation, variance, skewness and excess kurtosis of the posterior for β calculated under different methods—namely, the numerical quadrature based on $\pi(\beta | y = 1)$, and Monte Carlo integration leveraging the posterior samples from $(\beta | y = 1)$ generated by the data augmentation Gibbs sampler in Albert and Chib (1993), and the HMC in Algorithm 1, respectively.

	$E(\beta y, x)$	$\text{var}(\beta y, x)$	$\gamma_1(\beta y, x)$	$\gamma_2(\beta y, x)$
Integration via quadrature	7.94	36.97	0.96	0.82
Monte Carlo integration via Gibbs	6.96	27.02	0.80	0.35
Monte Carlo integration via HMC	7.83	35.82	0.95	0.82

representation of the SUN in equation (4) reached converge much rapidly and with an excellent mixing, the same MCMC settings were considered for both algorithms in order to facilitate comparison.

According to Figure 2 and Table 1, the HMC has excellent match with the functions and quantities obtained analytically, thus providing reassurance for the correctness of the derivations in Section 2.2. The data augmentation MCMC by Albert and Chib (1993) provides instead more evident differences, with a tendency to underestimate variance, skewness and heavy tails. This is due to the poor mixing of the data augmentation MCMC, which induces dependence via the full conditionals of the augmented data and the β parameter. Indeed, the effective sample size of the posterior samples produced by the data augmentation MCMC—computed with the function `effectiveSize` in the R library `coda`—is 162 over a total of 10000 samples. Although this poor mixing is surprising for a simplistic example based on a single observation from an intercept-only Bayesian probit regression, it shall be noticed that this

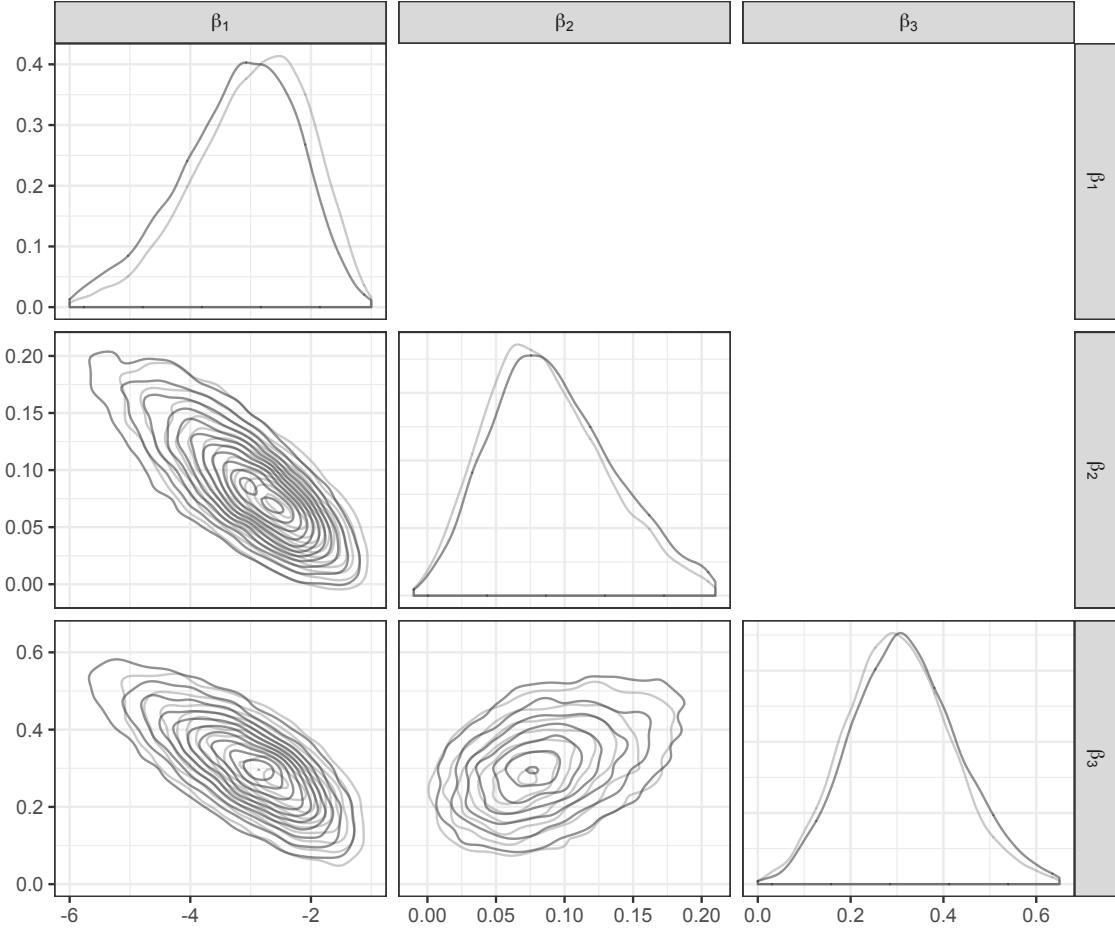


Fig. 3. Kernel density estimates of the marginal and bivariate posteriors for the regression coefficients in the Cushing study. These quantities are computed from the posterior samples of $(\beta | y, \mathbf{X})$ generated by the data augmentation Gibbs sampler in Albert and Chib (1993) (light grey), and the HMC in Algorithm 1 (dark grey).

data set is imbalanced since there is a single $y = 1$ and no cases of $y = 0$. The HMC has instead an effective sample size of 10000 over a total of 10000 samples, thereby providing the same mixing of an independent sampler. Indeed, the additive representation of a $SN(0, 100, 1)$ relies a linear combination of univariate Gaussians and truncated Gaussians, thus allowing tractable independent sampling.

3.2. Illustrative real-data applications

As a first real-data application, let us consider the **Cushings** data set from the R library **MASS**. These data refer to a medical study on the relation between the Cushing's syndrome and the over-secretion of cortisol by the adrenal gland. To address this goal, two covariates measuring the urinary excretion rates of two steroid metabolites—namely **Tetrahydrocortisone** and **Pregnanetriol**—are collected for $n = 27$ individuals along with the type of Cushing's syndrome. Here the focus is on the **carcinoma** type ($y = 1$) against the others ($y = 0$).

Figure 3 summarizes the marginal and the bivariate posteriors for $\beta = (\beta_1, \beta_2, \beta_3)^\top$ in the Bayesian probit regression $(y_i | \mathbf{x}_i, \beta) \sim \text{Bern}\{\Phi(\beta_1 + \beta_2 x_{i2} + \beta_3 x_{i3})\}$, $i = 1, \dots, n$, with x_{i2} and x_{i3} denoting

Table 2. Expectation, variance, skewness and excess kurtosis of the posteriors for the regression coefficients in the Cushing study. These quantities are calculated via Monte Carlo integration from the posterior samples of $(\beta | y, \mathbf{X})$ generated by the data augmentation Gibbs sampler in Albert and Chib (1993), and the HMC in Algorithm 1, respectively.

		$E(\beta y, x)$	$\text{var}(\beta y, x)$	$\gamma_1(\beta y, x)$	$\gamma_2(\beta y, x)$
β_1	Data augmentation Gibbs	-2.993	0.988	-0.629	0.498
	HMC additive SUN	-3.278	1.143	-0.713	0.764
β_2	Data Augmentation Gibbs	0.087	0.002	0.608	0.451
	HMC additive SUN	0.095	0.002	0.638	0.529
β_3	Data Augmentation Gibbs	0.303	0.013	0.208	0.168
	HMC additive SUN	0.322	0.014	0.295	0.208

the urinary excretion rates of the two metabolites measured for unit i . To evaluate the computational performance of the different routines in this application, the quantities in Figure 3 are derived from the posterior samples produced by the data augmentation MCMC, and by the HMC in Algorithm 1, based on a default $\beta \sim N(\mathbf{0}, 100 \cdot \mathbf{I}_3)$ prior, and the same MCMC settings in the simulation study. According to Figure 3, the two sampling mechanisms have comparable marginal and bivariate distributions, with the posterior for the coefficients associated with the urinary excretions of the two metabolites suggesting a positive effect on the chance of carcinoma. The HMC seems however to have an improved performance in exploring the parametric space, including tail areas. This is confirmed by the functionals of the posteriors for the coefficients in Table 2. Consistent with the illustrative simulation, the reasons of this improved performance can be found in the excellent mixing of the HMC, which has again an effective sample size of 10000 over a total of 10000 for all the sampled coefficients in $\beta = (\beta_1, \beta_2, \beta_3)^\top$, thus obtaining similar efficiency of an independent sampler. The effective sample sizes associated with the data augmentation MCMC are instead 434, 632, and 780, for β_1 , β_2 and β_3 , respectively.

To conclude the empirical assessments in real-data applications, Figure 4 summarizes the predictive performance for a large p and small n leukemia data set available in the R library `supclust`. Such data are a subset of the study conducted by Golub et al. (1999), and comprise information on the mRNA expression of $p - 1 = 250$ genes collected for $n = 38$ patients with two subtypes of Leukemia—namely AML ($y = 1$) and ALL ($y = 0$). Besides detecting those genes mostly associated with the two main subtypes of Leukemia, an overarching goal in these genetic studies is to predict the chance of a particular disease as a function of genes expressions. Consistent with this focus, Figure 4 summarizes the posterior predictive probabilities for each statistical unit $i = 1, \dots, 38$ obtained via a leave-one-out approach and a $\beta \sim N_{251}(\mathbf{0}, 100 \cdot \mathbf{I}_{251})$ prior. As discussed in Section 2.2.3, such quantities can be calculated with the exact expression in equation (8), or via Monte Carlo integration methods providing $\sum_{s=1}^S \Phi(\mathbf{x}_i^\top \beta^{(s)})/S$, with $\beta^{(1)}, \dots, \beta^{(S)}$ being samples from the posterior $(\beta | \mathbf{y}_{-i}, \mathbf{X}_{-i})$, $i = 1, \dots, n$. Such Monte Carlo approximations are computed for the two competing sampling schemes, and are

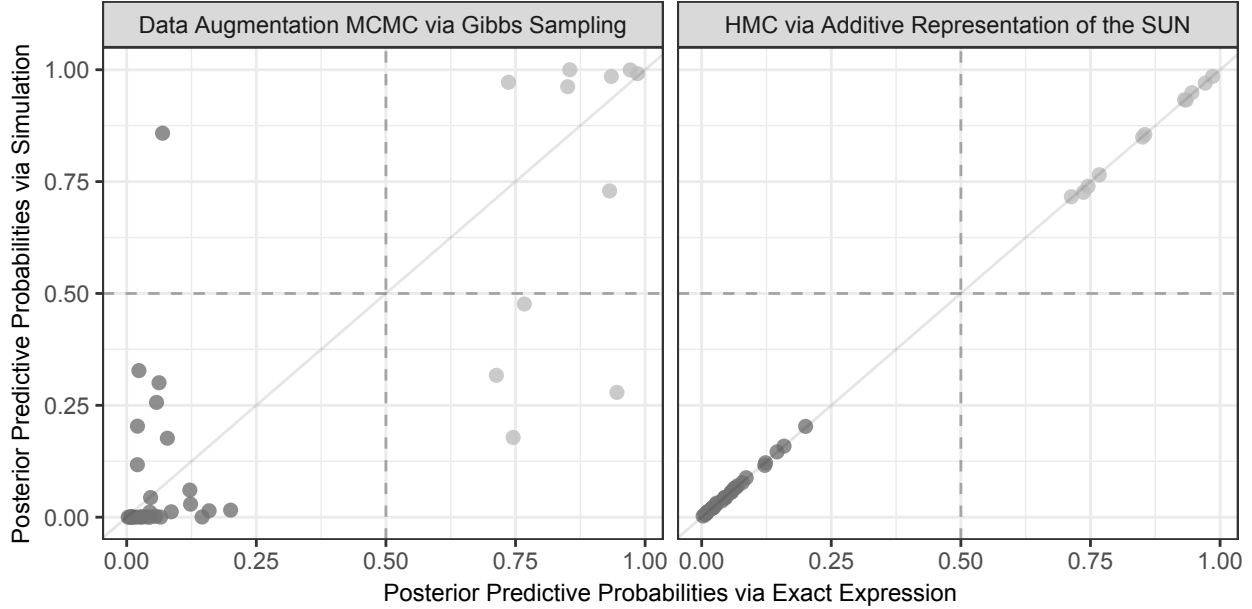


Fig. 4. Scatterplot comparing—in the Leukemia study—the leave-one-out posterior predictive probabilities $\text{pr}(y_{\text{new}} = 1 \mid \mathbf{y}, \mathbf{X}, \mathbf{x}_{\text{new}})$ calculated via the exact expression in (8) (x -axis), with those obtained under Monte Carlo integration (y -axis) based on the posterior samples from $(\boldsymbol{\beta} \mid \mathbf{y}, \mathbf{X})$. In the left panel the sampling scheme considered is the data augmentation Gibbs sampler in Albert and Chib (1993), whereas in the right panel the samples from $(\boldsymbol{\beta} \mid \mathbf{y}, \mathbf{X})$ are generated by the novel HMC in Algorithm 1. Dark grey refers to units with $y_i = 0$, whereas light grey characterizes units having $y_i = 1$, $i = 1, \dots, 38$.

compared with those obtained from the exact expression (8), taking an average of 1000 evaluations of the functions in (8) to avoid unstable results. According to Figure 4, there is almost perfect match between the posterior predictive probabilities computed via (8) and their Monte Carlo approximation based on the HMC. The Gibbs sampler provides different predictions, leading to decreased predictive performance. In fact, the posterior predictive probabilities computed from equation (8) and from the Monte Carlo approximation based on the HMC sampler provide perfect out-of-sample classification of the Leukemia subtypes, whereas the data augmentation MCMC fails for some units. Note that, among the 251 Gibbs chains, the minimum effective sample size is 29 and the median of the effective sample sizes is 1483. Calculating these quantities for the HMC provides instead a minimum of 8042 and a median of 10000—again comparable to independent samplers. Therefore, the poor mixing associated with popular MCMC has a major effect not only on posterior inference, but also on prediction.

4. Discussion

The apparent absence of conjugacy in Bayesian regression for binary responses has motivated a wide variety of different proposals to ease posterior inference and speed-up computations (e.g. Chopin and Ridgway, 2017). Such strategies either exploit data augmentations to obtain simple updating steps within an MCMC routine or rely on Gaussian approximations of the posterior to scale-up inference. As

recently discussed in Johndrow et al. (2017) both procedures have drawbacks in terms of efficiency and accuracy, thus motivating advances for posterior inference in Bayesian binary regression. This article takes a step in this direction by showing that the posterior in a Bayesian probit model with Gaussian priors belongs to a unified-skew normal class of variables (Arellano-Valle and Azzalini, 2006).

Such random variables have a well-studied normalizing constant, an analytical moment generating function, a tractable additive representation, and are closed under marginalization, conditioning and linear transformations, thus facilitating exact inference in small n studies as well as analytical derivation of the posterior predictive distribution and the development of a novel HMC sampler for efficient inference in large n applications. As shown in the empirical studies in Section 3, such routine has an excellent performance which is comparable to that of an independent sampler, and massively improves popular data augmentation MCMC sampling schemes. This methodology can lead to substantial computational gains not only for Bayesian probit regression but also for several hierarchical formulations relying on predictor-dependent latent binary data, covering models for density regression (Leonard, 1978; Ren et al., 2011; Rodriguez and Dunson, 2011), neural networks (Jordan et al., 1999), regression trees (Chipman et al., 2010), and hierarchical mixtures of experts (Jordan and Jacobs, 1994). Moreover, when binary regression serves as a dictionary function, sampling the dichotomous responses from the predictive distribution (8) induced by the Bayesian probit regression—instead of conditioning on the coefficients β via data augmentation MCMC—is also a possibility which could speed-up computations. Finally, the availability of the analytical marginal likelihood via the normalizing constant, and the novel conjugacy results in Section 2.2.4, can open new avenues for model selection and simple incorporation of skewness and heavy tails in prior specification—beyond the default Gaussian.

There are also several directions for additional advances. For instance, an improved study of the moment generating function of the SUN could facilitate the analytical calculation of relevant functionals without the need to sample from $(\beta | \mathbf{y}, \mathbf{X})$. On the same line, obtaining data transformations, or linear combinations of the parameters which allow $\Phi_n(\cdot)$ to factorize in lower-dimensional cumulative distribution functions having more stable and simpler evaluations, could substantially increase the range of applications which allow analytical inference and prediction, without sampling. Also approximations of the exact SUN posterior which preserve the main properties of this distribution but allow analytical inference are a possibility, partially related to variational Bayes ideas. As discussed in Section 1, the availability of an exact posterior having tractable stochastic representations and several closure properties could also motivate future theoretical studies on finite-sample and asymptotic properties of the posterior distribution.

References

Agresti, A. (2013) *Categorical Data Analysis (Third Edition)*. Wiley.

Albert, J. H. and Chib, S. (1993) Bayesian analysis of binary and polychotomous response data. *Journal of the American Statistical Association*, **88**, 669–679.

Arellano-Valle, R. B. and Azzalini, A. (2006) On the unification of families of skew-normal distributions. *Scandinavian Journal of Statistics*, **33**, 561–574.

Armagan, A. and Zaretsky, R. L. (2011) A note on mean-field variational approximations in Bayesian probit models. *Computational Statistics & Data Analysis*, **55**, 641–643.

Arnold, B. C. and Beaver, R. J. (2000) Hidden truncation models. *Sankhyā: The Indian Journal of Statistics, Series A*, **62**, 23–35.

Arnold, B. C., Beaver, R. J., Azzalini, A., Balakrishnan, N., Bhaumik, A., Dey, D., Cuadras, C. and Sarabia, J. M. (2002) Skewed multivariate models related to hidden truncation and/or selective reporting. *Test*, **11**, 7–54.

Azzalini, A. (1985) A class of distributions which includes the normal ones. *Scandinavian Journal of Statistics*, **12**, 171–178.

— (2013) *The Skew-normal and Related Families*. Cambridge University Press.

Azzalini, A. and Capitanio, A. (1999) Statistical applications of the multivariate skew normal distribution. *Journal of the Royal Statistical Society. Series B (Statistical Methodology)*, **61**, 579–602.

Azzalini, A. and Dalla Valle, A. (1996) The multivariate skew-normal distribution. *Biometrika*, **83**, 715–726.

Bazán, J. L., Branco, M. D. and Bolfarine, H. (2006) A skew item response model. *Bayesian Analysis*, **1**, 861–892.

Bliss, C. I. (1934) The method of probits. *Science*, **79**, 38–39.

— (1935) The calculation of the dosage-mortality curve. *Annals of Applied Biology*, **22**, 134–167.

Canale, A. (2011) Statistical aspects of the scalar extended skew-normal distribution. *Metron*, **69**, 279–295.

Chen, M.-H., Dey, D. K. and Shao, Q.-M. (1999) A new skewed link model for dichotomous quantal response data. *Journal of the American Statistical Association*, **94**, 1172–1186.

Chipman, H. A., George, E. I. and McCulloch, R. E. (2010) BART: Bayesian additive regression trees. *The Annals of Applied Statistics*, **4**, 266–298.

Choi, H. M. and Hobert, J. P. (2013) The Polya-Gamma Gibbs sampler for Bayesian logistic regression is uniformly ergodic. *Electronic Journal of Statistics*, **7**, 2054–2064.

Chopin, N. and Ridgway, J. (2017) Leave Pima Indians alone: Binary regression as a benchmark for Bayesian computation. *Statistical Science*, **32**, 64–87.

Consonni, G. and Marin, J.-M. (2007) Mean-field variational approximate Bayesian inference for latent variable models. *Computational Statistics & Data Analysis*, **52**, 790–798.

Cox, D. R. (1958) The regression analysis of binary sequences. *Journal of the Royal Statistical Society. Series B (Statistical Methodology)*, **20**, 215–242.

Dyke, G. and Patterson, H. (1952) Analysis of factorial arrangements when the data are proportions. *Biometrics*, **8**, 1–12.

Frühwirth-Schnatter, S. and Frühwirth, R. (2007) Auxiliary mixture sampling with applications to logistic models. *Computational Statistics & Data Analysis*, **51**, 3509–3528.

Genz, A. (1992) Numerical computation of multivariate normal probabilities. *Journal of Computational and Graphical Statistics*, **1**, 141–149.

— (1993) Comparison of methods for the computation of multivariate normal probabilities. *Computing Science and Statistics*, **25**, 400–405.

Golub, T. R., Slonim, D. K., Tamayo, P., Huard, C., Gaasenbeek, M., Mesirov, J. P., Coller, H., Loh, M. L., Downing, J. R., Caligiuri, M. A., Bloomfield, C. D. and Lander, E. S. (1999) Molecular classification of cancer: class discovery and class prediction by gene expression monitoring. *Science*, **286**, 531–537.

González-Farias, G., Domínguez-Molina, A. and Gupta, A. K. (2004) Additive properties of skew normal random vectors. *Journal of Statistical Planning and Inference*, **126**, 521–534.

Gupta, A. K., Aziz, M. A. and Ning, W. (2013) On some properties of the unified skew-normal distribution. *Journal of Statistical Theory and Practice*, **7**, 480–495.

Gupta, A. K., González-Farias, G. and Domínguez-Molina, J. A. (2004) A multivariate skew normal distribution. *Journal of Multivariate Analysis*, **89**, 181–190.

Holmes, C. C. and Held, L. (2006) Bayesian auxiliary variable models for binary and multinomial regression. *Bayesian Analysis*, **1**, 145–168.

Horrace, W. C. (2005) Some results on the multivariate truncated normal distribution. *Journal of Multivariate Analysis*, **94**, 209–221.

Jaakkola, T. S. and Jordan, M. I. (2000) Bayesian parameter estimation via variational methods. *Statistics and Computing*, **10**, 25–37.

Johndrow, J. E., Smith, A., Pillai, N. and Dunson, D. B. (2017) MCMC for imbalanced categorical data. *arXiv:1306.0040*.

Jordan, M. I., Ghahramani, Z., Jaakkola, T. S. and Saul, L. K. (1999) An introduction to variational methods for graphical models. *Machine Learning*, **37**, 183–233.

Jordan, M. I. and Jacobs, R. A. (1994) Hierarchical mixtures of experts and the EM algorithm. *Neural Computation*, **6**, 181–214.

Kotecha, J. H. and Djuric, P. M. (1999) Gibbs sampling approach for generation of truncated multivariate Gaussian random variables. *IEEE Proceedigns in Acoustics, Speech and Signal Processing*, **3**, 1757–1760.

Kuss, M. and Rasmussen, C. E. (2005) Assessing approximate inference for binary Gaussian process classification. *Journal of Machine Learning Research*, **6**, 1679–1704.

Leonard, T. (1978) Density estimation, stochastic processes and prior information. *Journal of the Royal Statistical Society. Series B (Statistical Methodology)*, **40**, 113–146.

Mi, X., Miwa, T. and Hothorn, T. (2009) `mvttnorm`: New numerical algorithm for multivariate normal probabilities. *The R Journal*, **1**, 37–39.

Miwa, T., Hayter, A. and Kuriki, S. (2003) The evaluation of general non-centred orthant probabilities. *Journal of the Royal Statistical Society. Series B (Statistical Methodology)*, **65**, 223–234.

Pakman, A. and Paninski, L. (2014) Exact Hamiltonian Monte Carlo for truncated multivariate Gaussians. *Journal of Computational and Graphical Statistics*, **23**, 518–542.

Polson, N. G., Scott, J. G. and Windle, J. (2013) Bayesian inference for logistic models using Pólya–Gamma latent variables. *Journal of the American Statistical Association*, **108**, 1339–1349.

Press, W. H., Teukolsky, S. A., Vetterling, W. T. and Flannery, B. P. (2007) *Numerical Recipes: The Art of Scientific Computing (Third Edition)*. Cambridge University Press.

Quarteroni, A., Sacco, R. and Saleri, F. (2010) *Numerical Mathematics (Second Edition)*. Springer Science & Business Media.

Ren, L., Du, L., Carin, L. and Dunson, D. B. (2011) Logistic stick-breaking process. *Journal of Machine Learning Research*, **12**, 203–239.

Rodriguez, A. and Dunson, D. B. (2011) Nonparametric Bayesian models through probit stick-breaking processes. *Bayesian Analysis*, **6**, 145–178.

Roy, V. and Hobert, J. P. (2007) Convergence rates and asymptotic standard errors for markov chain monte carlo algorithms for bayesian probit regression. *Journal of the Royal Statistical Society. Series B (Statistical Methodology)*, **69**, 607–623.

Rue, H., Martino, S. and Chopin, N. (2009) Approximate Bayesian inference for latent Gaussian models by using integrated nested Laplace approximations. *Journal of the Royal Statistical Society. Series B (Statistical Methodology)*, **71**, 319–392.

Spiegelhalter, D. J. and Lauritzen, S. L. (1990) Sequential updating of conditional probabilities on directed graphical structures. *Networks*, **20**, 579–605.

Wilhelm, S. and Manjunath, B. G. (2010) **tmvtnorm**: A package for the truncated multivariate normal distribution. *The R Journal*, **2**, 25–29.

Zobay, O. (2014) Variational Bayesian inference with Gaussian-mixture approximations. *Electronic Journal of Statistics*, **8**, 355–389.